Photoionization of the silicon divacancy studied by positron-annihilation spectroscopy

H. Kauppinen* and C. Corbel†
Institut National des Sciences et Techniques Nucléaires, Centre d'Etudes Nucléaires de Saclay, 91191 Gif-sur-Yvette Cedex, France

J. Nissilä, K. Saarinen, and P. Hautojärvi
Laboratory of Physics, Helsinki University of Technology, P.O. Box 1100, FIN-02015 HUT, Finland

(Received 3 October 1997)

The optical ionization of the silicon divacancy in 2-MeV electron-irradiated Si was studied by using positron-lifetime and positron-electron momentum distribution measurements under illumination with monochromatic light. Upon irradiation at room temperature, negative and neutral divacancies are detected in both float zone and Czochralski Si by positron-annihilation measurements in darkness. The positron-annihilation characteristics of the divacancy are determined as $\tau_d = 300(5)$ ps $= 1.35(2) \times \tau_b$, $S_d = 1.055(3) \times S_b$, and $W_d = 0.75(2) \times W_b$. Illumination at 15 K with monochromatic 0.70–1.30 eV light has a strong effect on the positron trapping rate to the divacancies. The results can be understood in terms of optical electron and hole emission from the electron levels $V_2^{-/0}$ and $V_2^{2-/-}$ of the divacancy. The changes in the positron trapping rate are due to the different sensitivities of the positron to the charge states V_2^0, V_2^-, and V_2^{2-}. The spectral shape of the positron trapping rate under illumination reveals an electron level at $E_v + 0.75$ eV, which is attributed to the ionization level $V_2^{2-/-}$ of the divacancy. [S0163-1829(98)10819-6]

I. INTRODUCTION

Point defects are created in the silicon lattice during the crystal growth as well as in the processing of the material, e.g., by ion implantation. To introduce and study simple point defects in Si in a controlled way, one generally uses electron irradiation. The most important defects created upon irradiation and room-temperature annealing are the divacancy, vacancy-oxygen complexes, and vacancy dopant-impurity pairs. The abundances of these defects depend on the oxygen and dopant concentrations in the material. Their structures and the electron levels in the forbidden gap have been investigated by electron paramagnetic resonance (EPR), infrared (IR) absorption, and deep-level transient spectroscopy (DLTS) measurements.[1,2]

Positron-annihilation spectroscopy[3–5] offers complementary information on vacancy defects in silicon and silicon-based systems. The positron lifetime and the momentum distribution of the annihilating positron-electron pair depend on the annihilation state of the positron. Positron trapping and annihilation at vacancies are manifested as an increase of the positron lifetime and as a narrowing of the e^+-e^- momentum distribution with respect to the free positron annihilation in the lattice. The positron trapping rate $\kappa = \mu c$ is proportional to the defect concentration c and it is sensitive to the charge state of the defect via the defect-specific positron trapping coefficient μ. Defect concentrations greater than or equal to 10^{14} cm^{-3} can be measured and there are no limitations as regards the electrical properties of the specimen. In addition, the chemical identity of the atoms involved in a defect, for example, impurity decoration, can be observed by means of the high-momentum tail of the e^+-e^- momentum distribution.

The ability of the positron-annihilation technique to probe the electron-irradiation-induced defects in Si is well established by many studies.[6] Mäkinen *et al.*[7] observed the isolated monovacancy in a negative charge state after electron irradiation at 20 K. Mascher, Dannefaer, and Kerr[8] investigated the positron trapping to the different charge states V_2^0, V_2^-, and V_2^{2-} of the divacancy and determined their positron trapping coefficients. They also observed shallow positron traps in n-type Si, which they associated with the vacancy-oxygen pairs or the A centers. The vacancy-phosphorus pair or the phosphorus E center was also studied by Mäkinen *et al.*[7] Recently, the divacancies and the decoration of vacancies by oxygen and other impurities have been studied by several authors with positron lifetime spectroscopy,[9,10] two-dimensional angular correlation of annihilation radiation technique,[11] and measurements of the high-momentum tail of the e^+-e^- momentum distribution.[12,13]

In this paper we combine positron-annihilation spectroscopy and photoexcitation to study the optical properties of the divacancy, thereby adding an important component to the study of defects in Si by positrons. Using the technique introduced earlier to study optically active defects in GaAs,[14,15] we measure the positron trapping rate to divacancies at 15 K under illumination with monochromatic (0.70–1.30)-eV light. We observe that, depending on the photon energy, the positron trapping rate to divacancies can be both enhanced and reduced by light and the maximum amplitude of the light-induced changes in the positron trapping is as high as a factor of 2. We show that these effects can be explained by the photoionization of the divacancy.

To separate the divacancy signal from the positron annihilation at impurity-related defects, we have combined the information obtained from positron lifetime and momentum distribution measurements. Such a method shows that, in addition to the divacancies, positrons annihilate also at vacancy-oxygen complexes, in agreement with earlier investigations.[8] To vary the relative concentrations of the two defects, we irradiated both float-zone (FZ) refined Si and

TABLE I. Electron-irradiated silicon samples and positron trapping rates to vacancies measured at 15 K. Sample $F1$ was cut from a FZ Si wafer ($\rho = 10^4\ \Omega$ cm, $[O] \leq 10^{15}\ cm^{-3}$) and samples $C1-C3$ from a B-doped CZ Si wafer ($\rho = 8-15\ \Omega$ cm, $[O] = 10^{18}\ cm^{-3}$). The second column shows the electron-irradiation fluences. The irradiations were performed with 2-MeV electrons at room temperature. The quantities shown in columns 3–5 are measured at 15 K and they are, respectively, the positron trapping rate $\kappa_{V\text{-O}}$ to vacancy-oxygen defects, positron trapping rate κ_{V_2} to divacancies in darkness, and the ratio of κ_{V_2} under 0.95-eV photoillumination to that under 0.70-eV photoillumination.

Sample	e^--irradiation fluence (cm^{-2})	Positron trapping rates to vacancies at 15 K		
		$\kappa_{V\text{-O}}$ (ns^{-1})	κ_{V_2} (ns^{-1}) in darkness	κ_{V_2} (0.95 eV)/κ_{V_2} (0.70 eV)
$F1$	1×10^{18}	0.8(5)	3.2(3)	2.0(2)
$C1$	3×10^{17}	2.6(3)	1.5(2)	2.8(5)
$C2$	1×10^{18}	3.0(5)	3.0(3)	2.6(6)
$C3$	5×10^{18}	6(1)	14(1)	2.0(3)

Czochralski (CZ) grown Si materials where the oxygen concentrations are different.

II. EXPERIMENTS AND DATA ANALYSIS

For the electron irradiations, four sample pairs were cut from (100) oriented FZ Si and CZ Si wafers, as shown in Table I. The FZ Si was undoped and slightly p type before irradiation ($\rho = 10^4\ \Omega$ cm). The CZ Si was boron doped and p type before irradiation ($\rho = 8-15\ \Omega$ cm). The oxygen-impurity concentrations are $[O] \leq 10^{15}\ cm^{-3}$ in FZ Si and $[O] = 1\times10^{18}\ cm^{-3}$ in CZ Si. The samples were irradiated with 2-MeV electrons at room temperature in a van de Graaff electron accelerator. One FZ Si sample ($F1$) was irradiated to an electron fluence $1\times10^{18}\ cm^{-2}$. Three CZ Si samples ($C1$, $C2$, and $C3$) were irradiated to electron fluences 3×10^{17}, 1×10^{18}, and $5\times10^{18}\ cm^{-2}$, respectively.

The electron-irradiated samples and unirradiated reference samples were subjected to positron lifetime and Doppler-broadening measurements at temperatures between 15 and 300 K. Two apparatuses were used. Samples $F1$ and $C2$ were measured with a 60-μCi ^{22}Na positron source in one apparatus where the time resolution of the positron lifetime spectrometer was 225 ps. Samples $C1$ and $C3$ were measured with a 40-μCi source in another apparatus where the time resolution was 250 ps. The source components (230 ps/5.4%, 500 ps/0.8%, and 1500 ps/0.15%) were subtracted from the positron lifetime spectra before further analysis. The Doppler-broadened annihilation line $L(E_\gamma)$ at 511 keV was measured with a high-purity (HP) Ge detector. The energy resolutions of the HP Ge detectors were 1.2 keV in both apparatuses.

The responses of the positron annihilation signals to the illumination were studied as follows.[14,15] The cryostats of both apparatuses were equipped with a quartz window to enable the back illumination on both samples of the sample sandwich during the measurements. The light obtained from a halogen lamp was monochromated [$\delta(h\nu) \leq 0.02$ eV] and guided on the samples by two branches of a trifurcated optical fiber. The illuminating photon flux was measured with a Si/Ge photodetector connected to the third branch of the optical fiber. The positron lifetime and the Doppler broadening were measured at 15 K under illumination with monochromatic light, as a function of the photon energy from 0.70 to 1.30 eV. At a photon energy of 0.95 eV the measurements were carried out as a function of the photon flux from 1×10^{13} to $1\times10^{16}\ cm^{-2}\ s^{-1}$. In all other illumination experiments the photon flux was $1\times10^{16}\ cm^{-2}\ s^{-1}$. At photon energies 0.70 and 0.95 eV (or 1.0 eV) the positron lifetime and the Doppler broadening were also measured as a function of temperature from 15 to 300 K.

The positron lifetime spectra $-(dn/dt) = \sum_{i=1}^{M} (I_i/\tau_i)\exp(-t/\tau_i)$ were analyzed with one component ($M = 1$) in the unirradiated samples and with two components ($M = 2$) in the electron-irradiated samples. Decomposition to three components was not possible because of the proximity of the different lifetimes. The average positron lifetime τ_{ave}, which coincides with the center of mass of the lifetime spectrum, is calculated from the fitted lifetimes τ_i and their intensities I_i as

$$\tau_{\text{ave}} = \int_0^\infty t\left(\frac{-dn}{dt}\right)dt = \sum_{i=1}^{M} I_i\tau_i . \quad (1)$$

The average positron lifetime is insensitive to uncertainties in the decomposition procedure.

The Doppler broadening ΔE_γ of the 511-keV annihilation $L(E_\gamma)$ line is related to the momentum distribution of the annihilating positron-electron pair by $\Delta E_\gamma = cp_z/2$, where p_z is the momentum component along the line of emission of the two annihilation photons. We characterize the e^+-e^- momentum distribution with the usual shape parameters S and W. The S and W parameters are the fractions of positrons annihilating with electrons in the low-momentum range $p_z = (0-2.8)\times10^{-3} m_0 c$ and in the high-momentum range $p_z = (11-20)\times10^{-3} m_0 c$, respectively.

III. RESULTS

A. Unirradiated Si

In unirradiated FZ and CZ Si the positron lifetime is 221 ps at 15 K and it increases slightly to 222 ps at 300 K. The S and W parameters in the unirradiated samples are $S_b = 0.4548(2)$ and $W_b = 0.0232(1)$, respectively, at temperatures between 15 and 300 K. In the following, the S and W parameters are presented as ratios S/S_b and W/W_b, respec-

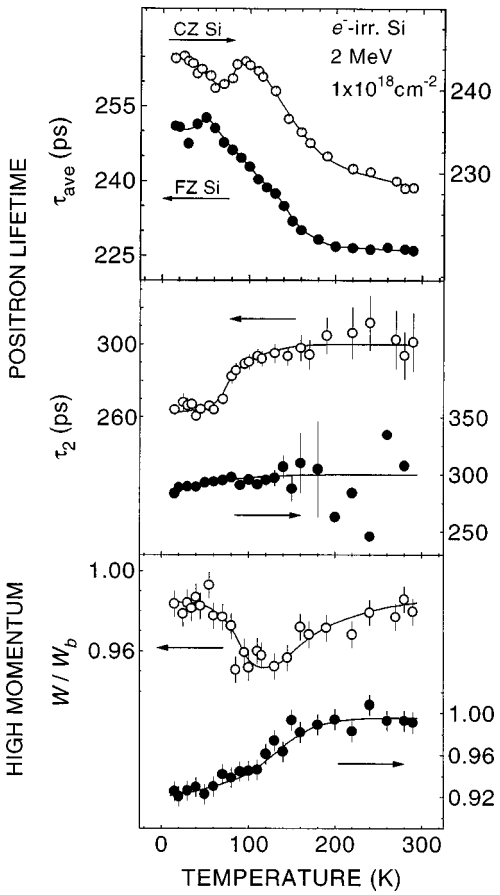

FIG. 1. Average positron lifetime τ_{ave}, the second component τ_2 of the two-component lifetime spectrum, and the high-momentum parameter W of the Doppler-broadened annihilation line vs measurement temperature in electron-irradiated Si: (●) FZ Si (sample $F1$) and (○) CZ Si (sample $C2$). The solid lines are guides to the eye.

tively. In the unirradiated samples, neither the positron lifetime nor the S or W parameters showed any response to illumination at the photon energies between 0.70 and 1.30 eV.

B. Electron-irradiated FZ and CZ Si at 15–300 K in darkness

The description of the temperature dependence of the positron lifetime and the Doppler broadening in the electron-irradiated samples can be divided in two temperature ranges 150–300 and 15–150 K. Between 150 and 300 K all irradiated samples $F1$ and $C1-C3$ show rather similar behavior and the results can be summarized as follows (Fig. 1). The average positron lifetime τ_{ave} is higher than the value 221–222 ps in unirradiated Si and it increases as the temperature decreases. The second lifetime component τ_2 is 300(5) ps. The S parameter increases and W parameter decreases when temperature decreases.

Between 15 and 150 K the temperature dependences of the positron lifetime and the Doppler broadening are more complex and we describe the results sample by sample. The S parameter shows behavior that is consistent with that of W and we discuss here only the latter. The FZ and CZ Si materials are compared in Fig. 1, where the results are shown for samples $F1$ and $C2$, both irradiated to the electron fluence of 1×10^{18} cm^{-2}. In FZ Si sample $F1$ the average positron lifetime τ_{ave} continues to increase as the temperature decreases from 150 to 50 K, below which it is almost constant except for a slight dip at 30 K. The second lifetime component τ_2 decreases somewhat as the temperature decreases and it is 285 ps at 15 K. The W parameter decreases in a continuous way as the temperature decreases from 150 to 15 K. In CZ Si sample $C2$, the average positron lifetime τ_{ave} increases as the temperature decreases from 150 to 90 K and then it decreases when the temperature decreases from 90 to 60 K, below which it increases again. The decrease of τ_{ave} between 60 and 90 K is accompanied by a rapid decrease in τ_2 and at 15 K, τ_2 is 265 ps. The W parameter decreases as the temperature decreases from 150 to 90 K, below which it increases strongly, and at 15 K W is at the same level as that at 300 K.

In CZ Si sample $C1$, the behaviors of τ_{ave}, τ_2, and W at temperatures between 15 and 150 K are similar to those in sample $C2$. At 15 K, τ_2 has decreased to 250 ps and W is at a level even higher than that at 300 K. In sample $C3$, τ_{ave} increases and τ_2 decreases in a continuous way as the temperature decreases from 150 to 15 K. The W parameter decreases as the temperature decreases from 150 to 90 K, below which it increases again. At 15 K, τ_2 is 280 ps and the W parameter is almost at the same level as that at 300 K.

C. Electron-irradiated FZ and CZ Si under (0.70–1.30)-eV illumination

The illumination has a strong effect on the positron lifetime and Doppler broadening at 15 K in all electron-irradiated samples. The FZ and CZ Si materials are compared in Fig. 2, where the results are shown for samples $F1$ and $C2$ irradiated to the fluence of 1×10^{18} cm^{-2}. The amplitudes of the changes in the average positron lifetime τ_{ave} vs photon energy are around 15 ps. This is much larger than the experimental uncertainty $\Delta\tau_{ave}=0.3$ ps of the average lifetime.

In FZ Si sample $F1$ under illumination with 0.70-eV light, τ_{ave} is 2 ps above the value τ_{ave}^{dark} measured in darkness. As the photon energy increases above 0.75 eV, τ_{ave} increases rapidly and levels off at 0.90 eV, where it is 17 ps above τ_{ave}^{dark}. As the photon energy increases above the Si band gap $E_g=1.17$ eV, τ_{ave} decreases rapidly but stays 7 ps above τ_{ave}^{dark} when the photon energy is 1.30 eV. The second lifetime component τ_2 shows a pattern similar to that in τ_{ave}. In CZ Si sample $C2$, we observe the same behavior of τ_{ave} and τ_2 vs photon energy: τ_{ave} and τ_2 increase when the photon energy increases above 0.75 eV and they decrease near the band-gap energy. There are, however, two marked differences with respect to FZ Si. First, the τ_{ave} vs photon energy curve is now shifted downward with respect to τ_{ave}^{dark}. At 0.70 eV, τ_{ave} is 7 ps below τ_{ave}^{dark} and between 0.90 and 1.0 eV, τ_{ave} is 9 ps above τ_{ave}^{dark}. The second difference is that in CZ Si the decrease of τ_{ave} near the band-gap energy begins already at 1.0 eV and it continues until 1.25–1.30 eV.

In CZ Si samples $C1$ and $C3$, the τ_{ave} and τ_2 vs photon energy curves have shapes similar to those in sample $C2$, but the levels of the curves with respect to the values in darkness are different. In sample $C1$, at 0.70 eV, τ_{ave} is 2 ps below

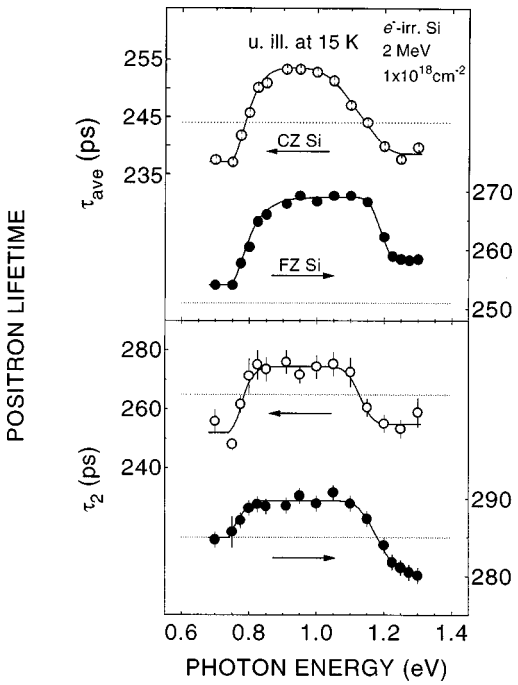

FIG. 2. Positron lifetime in electron-irradiated Si at 15 K under illumination with monochromatic light. The photon flux is 1×10^{16} cm^{-2} s^{-1}. The average positron lifetime τ_{ave} and the long lifetime component τ_2 are presented as a function of the illumination photon energy: (●) FZ Si (sample $F1$) and (○) CZ Si (sample $C2$). The dotted lines show the positron lifetime in darkness at 15 K. The solid lines are guides to the eye.

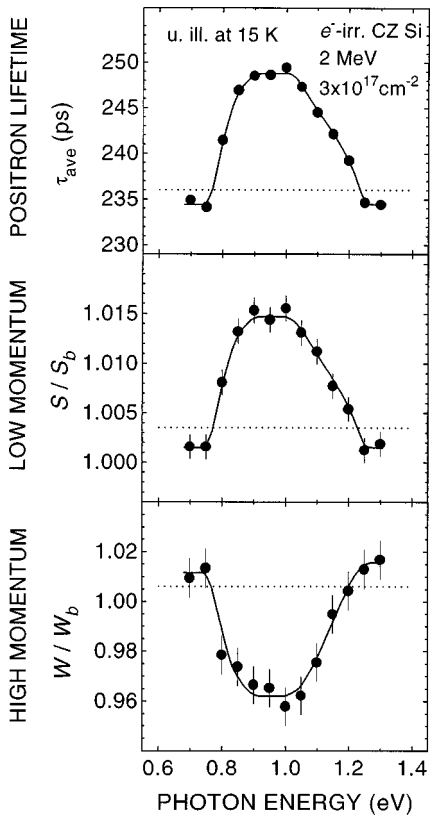

FIG. 3. Positron lifetime and Doppler broadening measured in the electron-irradiated CZ Si sample $C1$ at 15 K under illumination with monochromatic light. The photon flux is 1×10^{16} cm^{-2} s^{-1}. The average positron lifetime τ_{ave} and the S and W parameters are presented as a function of the illumination photon energy. The dotted lines show the values of τ_{ave}, S, and W measured in darkness at 15 K. The solid lines are guides to the eye.

τ_{ave}^{dark} and between 0.90 and 1.0 eV, τ_{ave} is 12 ps above τ_{ave}^{dark}. In sample $C3$, at 0.70 eV, τ_{ave} is 10 ps below τ_{ave}^{dark} and between 0.90 and 1.0 eV, τ_{ave} is 4 ps above τ_{ave}^{dark}. In CZ Si, the τ_{ave} vs photon energy curve thus shifts more and more downward with respect to τ_{ave}^{dark} when the electron-irradiation fluence increases. The lowest value $\tau_2=242$ ps of the second lifetime component in CZ Si is found in sample $C1$ under 0.70-eV illumination. The highest value $\tau_2=288$ ps in CZ Si is observed in sample $C3$ under (0.90–1.0)-eV illumination.

The Doppler-broadening parameters S and W show also strong responses to the illumination at 15 K. In all irradiated samples, S increases and W decreases when τ_{ave} increases. Figure 3 shows this behavior in sample $C1$. Moreover, the correlations $S(\tau_{ave})$ and $W(\tau_{ave})$ measured under illumination at 15 K are straight lines. This property is discussed in Sec. IV B 3.

The flux dependence of the positron annihilation signals was investigated at a photon energy of 0.95 eV. Figure 4 shows that in sample $C1$, τ_{ave}, S, and W level off at a photon flux of 1×10^{15} cm^{-2} s^{-1}. We found that the photon flux of 1×10^{16} cm^{-2} s^{-1} was sufficient to drive the illumination effects in saturation in all samples.

Figure 5 shows the temperature dependence of τ_{ave} under illumination in samples $F1$ (1.0 eV) and $C2$ (0.70 and 0.95 eV). The strongest response to illumination is observed at 15 K, above which the effects decrease. As temperature increases above 220 K, the effect of illumination is no longer visible. Similar behaviors were observed in samples $C1$ and $C3$.

No metastability was observed in the illumination effects. This was tested in CZ Si sample $C2$. The sample was first annealed at 300 K and then illuminated for 1 h at 15 K, after which the light was switched off and the positron lifetime and Doppler broadening were measured in darkness at 15 K. After such illuminations with 0.70-, 0.95-, or 1.25-eV photons, τ_{ave}, S, and W were the same as the respective values in darkness before any illumination.

IV. POSITRON TRAPPING TO DIVACANCIES AND VACANCY-OXYGEN DEFECTS

In the unirradiated material, the positron lifetime is 221 ps, which is the free positron lifetime τ_b in the Si lattice.[7] In the unirradiated material positrons thus annihilate in the Bloch state in the Si lattice and the parameters S_b and W_b are those of the lattice. In electron-irradiated FZ and CZ Si, the result $\tau_{ave}>\tau_b$ indicates that positrons are trapped at irradiation-induced vacancy defects. In the following, we show that there are two defects that act as the dominant positron traps.

A. Defect annihilation characteristics τ_d, S_d, and W_d

To determine the number of defects and their positron annihilation characteristics we use the following two methods.

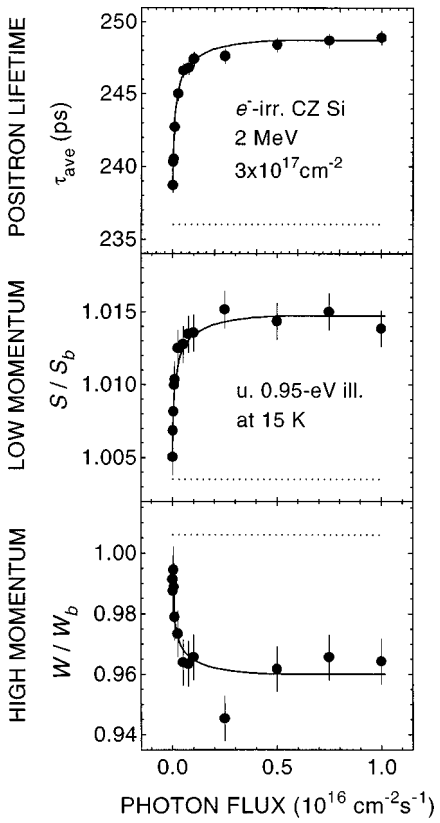

FIG. 4. Positron lifetime and Doppler broadening measured in the electron-irradiated CZ Si sample $C1$ at 15 K under illumination with 0.95-eV light. The average positron lifetime $\tau_{\rm ave}$ and the S and W parameters are presented as a function of the illumination photon flux. The dotted lines show the values of $\tau_{\rm ave}$, S, and W measured in darkness at 15 K. The solid lines are guides to the eye.

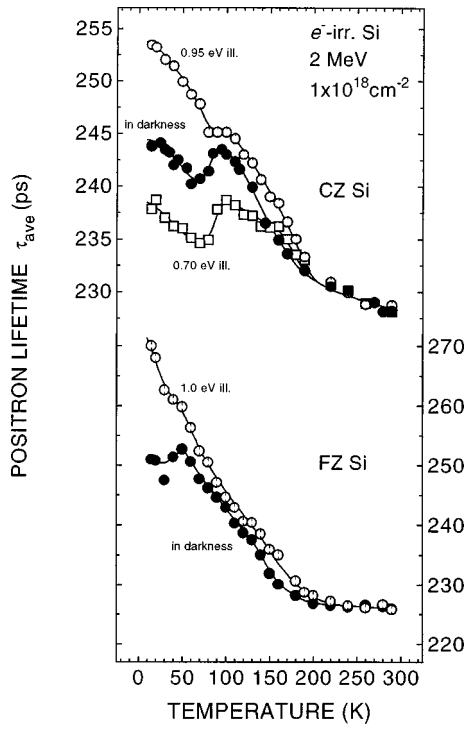

FIG. 5. Average positron lifetime $\tau_{\rm ave}$ in darkness and under illumination vs the measurement temperature in electron-irradiated Si. FZ Si sample $F1$, (●) in darkness and (○) under 1.0-eV illumination, CZ Si sample $C2$, (●) in darkness, (○) under 0.95-eV illumination, and (□) under 0.70-eV illumination. The solid lines are guides to the eye.

First, we calculate the so-called model bulk lifetime $\tau_{\rm mod}=(I_1/\tau_1+I_2/\tau_2)^{-1}$ from the two fitted lifetimes and their intensities. If $\tau_{\rm mod}=\tau_b$, there is only one positron trap and the two-component fit is physically meaningful. The presence of more than one positron trap is manifested as $\tau_{\rm mod}>\tau_b$. In the measurements performed in darkness between 150 and 300 K, we found that $\tau_{\rm mod}=222$–225 ps $\approx\tau_b$. As the temperature decreases below 150 K, $\tau_{\rm mod}$ increases in all samples and it is 230–265 ps $>\tau_b$, depending on the sample and the illumination conditions.

Second, we use the property that the three mean annihilation quantities $F^a\in[F^1=\tau_{\rm ave},\ F^2=S,\ F^3=W]$ can be expressed as linear functions of annihilations states

$$F^a=\eta_b F^a_b+\sum_{j=1}^{N}\eta_{dj}F^a_{dj}\quad\text{with}\quad\eta_b+\sum_{j=1}^{N}\eta_{dj}=1,\qquad(2)$$

where the subscript b corresponds to the free annihilation state in the lattice, the subscripts $dj=d1, d2, \ldots, dN$ correspond to N defect states, and η_b and η_{dj} are the fractions of positrons annihilating in the corresponding states. This relation can be investigated by plotting the measured data as F^a vs $F^{a'\neq a}$, that is, S vs $\tau_{\rm ave}$, W vs $\tau_{\rm ave}$, or S vs W. One notes from Eq. (2) that when only one type of positron trap exists, the $F^a(F^{a'})$ functions are linear. The nonlinearity of the experimental $F^a(F^{a'})$ data is a clear indication of the presence of at least two different types of positron traps. One should note that the experimental $F^a(F^{a'})$ data can form a straight line even in the presence of two positron traps, as we shall see in Sec. IV B 3. Therefore, to confirm that there is only one type of defect that traps positrons, one should also have $\tau_{\rm mod}=\tau_b$.

The $S(\tau_{\rm ave})$ and $W(\tau_{\rm ave})$ plots are presented in Figs. 6 and 7, respectively, for the data measured in darkness between 15 and 300 K and under (0.70–1.30)-eV illumination at 15 K. The data points that are closest to the bulk values (S_b,τ_b) and (W_b,τ_b) correspond to measurements at 300 K. In the temperature range 150–300 K, where the second lifetime component is $\tau_2=300(5)$ ps, the $S(\tau_{\rm ave})$ and $W(\tau_{\rm ave})$ data fall on straight lines that are common to all the electron-irradiated samples. As in addition $\tau_{\rm mod}=\tau_b$, we can conclude that in the range 150–300 K there is only one type of vacancy defect $d1$ that traps positrons and the characteristic positron lifetime of this defect is $\tau_{d1}=300$ ps. By extrapolating the $S(\tau_{\rm ave})$ and $W(\tau_{\rm ave})$ data to 300 ps we obtain the characteristic S and W values of this vacancy defect as $S_{d1}=1.055(3)\times S_b$ and $W_{d1}=0.75(2)\times W_b$.

The temperature range 15–150 K offers additional effects. As temperature decreases from 150 to 15 K, the $S(\tau_{\rm ave})$ data in Fig. 6 and even more clearly the $W(\tau_{\rm ave})$ data in Fig. 7 deviate from the straight lines observed at 150–300 K. In samples $C1$ and $C2$ the deviation from the straight lines is particularly abrupt when temperature decreases from 90 to 15 K. Such a nonlinear behavior of $S(\tau_{\rm ave})$ and $W(\tau_{\rm ave})$, further confirmed by the observation $\tau_{\rm mod}>\tau_b$, indicates the presence of at least two types of positron traps. We notice

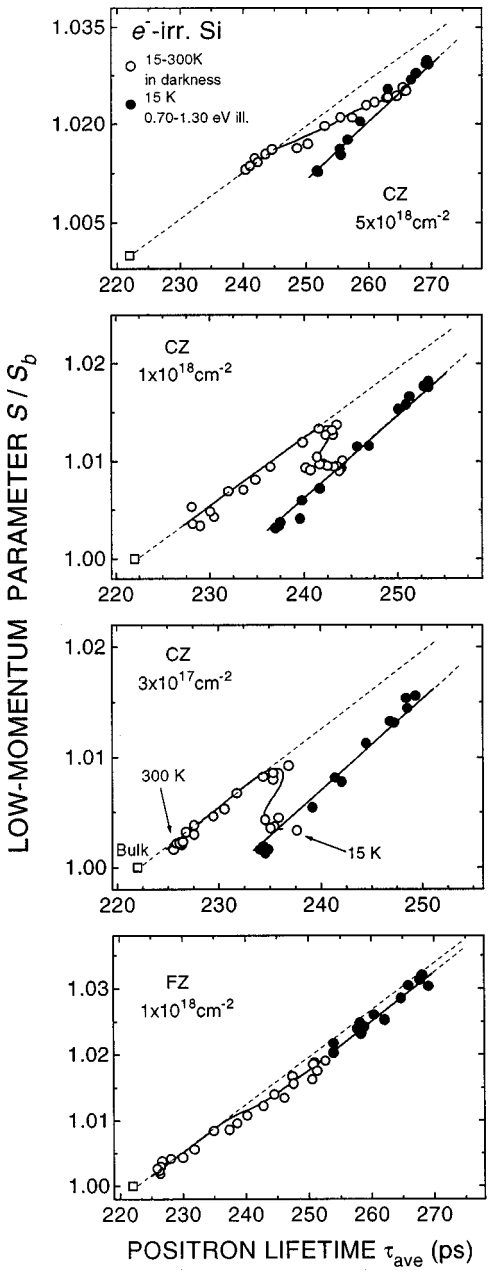

FIG. 6. Low-momentum parameter S measured in electron-irradiated FZ Si (sample $F1$) and CZ Si (samples $C1-C3$) presented as a function of the average positron lifetime τ_{ave}: (○) measurements in darkness at temperatures between 15 and 300 K and (●) measurements under (0.70–1.30)-eV photoillumination at 15 K. The dashed lines are extrapolated to the divacancy V_2. The solid lines are guides to the eye. The determination of the defect states is discussed in the text.

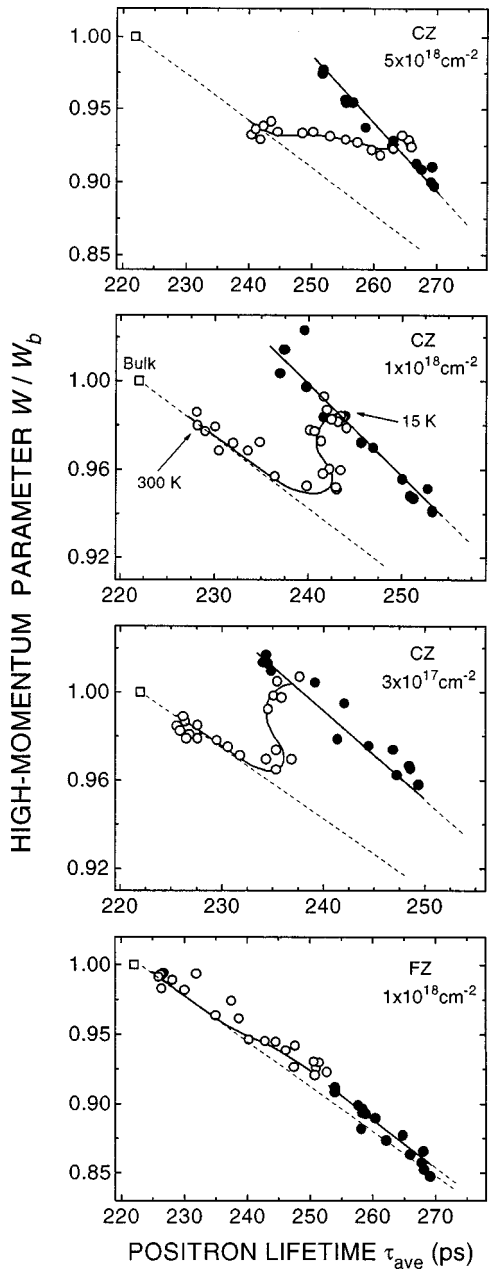

FIG. 7. High-momentum parameter W measured in electron-irradiated FZ Si (sample $F1$) and CZ Si (samples $C1-C3$) presented as a function of the average positron lifetime τ_{ave}. The meanings of the symbols are as in Fig. 6.

also that the decreasing of τ_2 below 300 ps, when temperature decreases from 150 to 15 K, correlates with the nonlinearity of $S(\tau_{\text{ave}})$ and $W(\tau_{\text{ave}})$. Obviously, the variations in signal τ_2, whether as a function of temperature or electron-irradiation fluence, result from a combination of different defect-specific positron lifetimes τ_{dj}. Below we show that the results can be understood by positron trapping to two defects, namely, to the defect $d1$ determined above and to another defect $d2$.

To estimate the positron lifetime τ_{d2} at the defect $d2$, we use the results obtained under illumination at 15 K, where the variations of the defect-related lifetime component τ_2 can also be ascribed to the mixing of two lifetimes τ_{d1} and τ_{d2}. The lowest value of τ_2 is measured in sample $C1$ under 0.70-eV illumination at 15 K and it is $\tau_2=242$ ps. In this measurement we have $\tau_{\text{mod}}=230$ ps$>\tau_b$, which indicates that the value $\tau_2=242$ ps is still a mixture of τ_{d1} and τ_{d2} and we can infer that $\tau_{d2}<242$ ps. On the other hand, the behavior of the $S(\tau_{\text{ave}})$ and $W(\tau_{\text{ave}})$ data in Figs. 6 and 7, respectively, implies that the defect state $d2$ is distinctly different from the Si lattice and we must thus have $\tau_{d2}>\tau_b$. Within the constraints 221 ps$<\tau_{d2}<242$ ps, we assign for the defect $d2$ a characteristic positron lifetime $\tau_{d2}=230(10)$ ps.

Once the positron lifetime τ_{d2} at the defect $d2$ is known,

we can determine its characteristic momentum parameters S_{d2} and W_{d2} by using the method presented in Ref. 16. We assume that detrapping of positrons from the defects does not occur. The second lifetime component can be approximated by an average of τ_{d1} and τ_{d2} as

$$\tau_2=\frac{\kappa_{d1}}{\kappa_{d1}+\kappa_{d2}}\,\tau_{d1}+\frac{\kappa_{d2}}{\kappa_{d1}+\kappa_{d2}}\,\tau_{d2}, \tag{3}$$

weighted, respectively, by the positron trapping rates κ_{d1} and κ_{d2} to the two defects. The total positron trapping rate $\kappa=\kappa_{d1}+\kappa_{d2}$ is

$$\kappa=\lambda_b\,\frac{\tau_{\rm ave}-\tau_b}{\tau_2-\tau_{\rm ave}}, \tag{4}$$

where $\lambda_b=\tau_b^{-1}$ is the annihilation rate in the lattice. The trapping rates κ_{d1} and κ_{d2} are related to the annihilation fractions η_b, η_{d1}, and η_{d2} in Eq. (2) by the formulas

$$\eta_b=\lambda_b/(\lambda_b+\kappa_{d1}+\kappa_{d2}), \tag{5}$$

$$\eta_{d1}=\kappa_{d1}/(\lambda_b+\kappa_{d1}+\kappa_{d2}), \tag{6}$$

$$\eta_{d2}=\kappa_{d2}/(\lambda_b+\kappa_{d1}+\kappa_{d2}). \tag{7}$$

We use in our analysis the positron lifetime and Doppler-broadening data measured at 15 K. At this temperature, positron detrapping from any defect is negligible. The positron trapping rates κ_{d1} and κ_{d2} can be solved from Eqs. (3) and (4) and they are presented below in Sec. IV B 3. The annihilation fractions η_{d1} and η_{d2} are then calculated from Eqs. (6) and (7), which completes the information necessary to solve the characteristic parameters S_{d2} and W_{d2} from Eq. (2). From samples $F1$ and $C1-C3$, we obtain $S_{d2}=(0.984,\ 0.987,\ 0.981,$ and $0.982)\times S_b$ and $W_{d2}=(1.15,\ 1.12,\ 1.18,$ and $1.20)\times W_b$. The values in the different samples are similar, which justifies the model of the two defects. We calculate the characteristic S and W parameters of the 230-ps defect as averages of the values in the four samples and we obtain $S_{d2}=0.984(3)\times S_b$ and $W_{d2}=1.16(4)\times W_b$.

B. Properties of the defects

In the following, we discuss the properties and the identification of the 300-ps and 230-ps defects.

1. Divacancy V_2

The positron-annihilation characteristics $\tau_{d1}=300(5)$ ps, $S_{d1}=1.055(3)\times S_b$, and $W_{d1}=0.75(2)\times W_b$ of the defect $d1$ are, within error bars, the same as the values $\tau_d=300(5)$ ps, $S_d=1.052(3)\times S_b$, and $W_d=0.78(2)\times W_b$ we obtained in our earlier work[17] for the divacancy in proton-implanted n-type chemically vapor deposited Si. The parameters $\tau_{d1}=300$ ps, $S_{d1}=1.055\times S_b$, and $W_{d1}=0.75\times W_b$ are close to the recent theoretical values $\tau_d=299$ ps, $S_d=1.051\times S_b$, and $W_d=0.76\times W_b$ calculated for the divacancy in (100) crystal orientation by Hakala, Puska, and Nieminen.[18] The parameters $\tau_{d1}=1.35(2)\times\tau_b$ and $S_{d1}=1.055\times S_b$ are also clearly higher than the values $\tau_d=(1.1-1.2)\times\tau_b$ and $S_d=(1.02-1.03)\times S_b$ usually assigned for monovacancy-type defects in semiconductors. We conclude that the 300-ps defect found in electron-irradiated FZ and CZ Si is the silicon divacancy V_2.

The observation of divacancies in electron-irradiated FZ and CZ Si is expected. It is known from EPR measurements that electron irradiation and room-temperature annealing creates divacancies and vacancy-impurity pairs in Si.[1,19,20] In FZ Si, the impurity concentration is low and the divacancy is the dominant positron trap at all temperatures. In CZ Si, both divacancies and vacancy-impurity complexes are formed. The divacancy is the dominant positron trap in the high-temperature range also in CZ Si, but as we shall see below, at low temperatures positrons are trapped at both divacancies and vacancy-impurity complexes.

Mascher, Dannefaer, and Kerr[8] and Avalos and Dannefaer[21] have assigned a characteristic positron lifetime $\tau_d=290-320$ ps for the divacancy, in good agreement with our value $\tau_{d1}=300(5)$ ps. Avalos and Dannefaer[21] have also reported a value $S_d=1.067(3)\times S_b$ for the characteristic S parameter of the divacancy in electron-irradiated FZ Si, which is somewhat higher than the value $S_{d1}=1.055(3)\times S_b$ we obtain for the divacancy.

In earlier studies values such as $S_d=1.034\times S_b$ have been reported for the divacancy (e.g., Ref. 31). These estimates are based on Doppler-broadening measurements in ion-implanted Si after a high implantation dose. In this type of experiments both the defect-type trapping positrons and the trapping fractions cannot be determined unambiguously because the contributions of various positron states to the annihilation line shape cannot be decomposed using Doppler-broadening data alone. Hence the estimated values of S_d may be inaccurate and the result $S_d=1.034\times S_b$ represents rather the lower limit of the S parameter at the divacancy. By combining positron lifetime and Doppler-broadening data as explained above or in earlier works (e.g., Ref. 21 or 32) we can (i) conclude that in the temperature range 150–300 K divacancies act as the only positron traps in our samples and (ii) determine the trapping fractions. We thus obtain more reliable values for the S parameter at the divacancy in Si than in the earlier studies (e.g., Ref. 31), where only Doppler-broadening experiments have been used.

2. Vacancy-oxygen complex

In the low-temperature range 15–150 K there exist two positron traps: the divacancy V_2 characterized above and another defect $d2$. The positron annihilation characteristics of the defect $d2$ are $\tau_{d2}=230(10)$ ps, $S_{d2}=0.984(3)\times S_b$, and $W_{d2}=1.16(4)\times W_b$. The positron lifetime ratio $\tau_{d2}/\tau_b=1.04(4)$ tells that the defect has an open volume, which is smaller than that in a monovacancy. On the other hand, for this defect $S_{d2}<S_b$ and $W_{d2}>W_b$, which means that the e^+-e^- momentum distribution at the 230-ps defect $d2$ is broader than that in the Si lattice. Theoretically, one would expect the e^+-e^- momentum distribution at an open-volume defect to be narrower than that in the Si lattice. Therefore, the 230-ps defect $d2$ cannot be a pure vacancy, but the momentum signal must reflect an impurity atom attached to the vacancy. We attribute this behavior to the oxygen decoration of the vacancy. The broadening of the e^+-e^- momentum distribution with respect to that in the Si lattice is observed in oxygen-rich environments such as SiO_2 and oxygen clusters

in Si.[6,22] The most abundant impurity in the CZ Si samples is oxygen and the effect of the 230-ps defect is much smaller in FZ Si where the oxygen concentration is low. In conclusion, we identify the 230-ps defect as a vacancy-oxygen complex V-O.

A variety of oxygen-related defects have been identified in electron-irradiated CZ Si by EPR measurements, such as the vacancy-oxygen pair or the A center,[20] the divacancy-carbon-oxygen complex V_2-CO,[23] and higher-order vacancy-oxygen complexes V_2-O, V_2-O_2, etc.[24] According to EPR measurements, the most abundant of these defects is the A center. Its structure is that of a nearly substitutional oxygen atom and it contains a small open volume. The 230-ps defect measured by positron annihilation, containing a small volume and oxygen, is most probably the A center.

3. Positron trapping rates κ_{V_2} and $\kappa_{V\text{-}O}$ and the defect charge states

The positron trapping rate κ_d to a defect state is defined as $\kappa_d=\mu_d c_d$, where c_d is the defect concentration and μ_d is the defect-specific positron trapping coefficient. If the trapping coefficient μ_d is known, the positron trapping rate κ_d can be used for deducing the defect concentration c_d. We calculate the positron trapping rates to the 300-ps and 230-ps defects from the $S(\tau_{\rm ave})$ and $W(\tau_{\rm ave})$ data of Figs. 6 and 7, respectively, by using Eqs. (2), (6), and (7). In all samples $F1$ and $C1-C3$ the $S(\tau_{\rm ave})$ and $W(\tau_{\rm ave})$ data, measured as a function of temperature and under illumination, give consistent results. This gives further justification for the model of two defects and the values of the defect parameters. In the following, the presented trapping rates are averages of the two values determined from the $S(\tau_{\rm ave})$ and $W(\tau_{\rm ave})$ data.

We first examine qualitatively the response of the positron trapping rates κ_{V_2} (divacancies) and $\kappa_{V\text{-O}}$ (vacancy-oxygen complexes) to photoillumination at 15 K. We see in Figs. 6 and 7 that in all samples the $S(\tau_{\rm ave})$ and $W(\tau_{\rm ave})$ data measured under (0.70–1.30)-eV illumination show a linear behavior. Moreover, the lines on which the data points are located go through the divacancy points (S_{d1}, τ_{d1}) and (W_{d1}, τ_{d1}). The equation of such lines in the S-$\tau_{\rm ave}$ and W-$\tau_{\rm ave}$ planes is $\eta_{d2}=\text{const}\times\eta_b$. This, when combined with Eqs. (5) and (7), means that the positron trapping rate $\kappa_{V\text{-O}}$ to the vacancy-oxygen defects is constant. The illumination thus affects only the positron trapping rate κ_{V_2} to divacancies, whereas the trapping rate to vacancy-oxygen defects remains the same under illumination and in darkness. We shall study this interesting result, which can be ascribed to the photoionization of the divacancy, below in Secs. V A–V D.

The temperature dependence of κ_{V_2} measured in darkness can be used to determine the charge state of the divacancy. After the irradiations, the samples are highly resistive and the Fermi level E_f is close to the middle of the band gap. All defects can be expected to remain in their charge states in the temperature range 15–300 K. Hence the variations in the positron trapping rate $\kappa_d=\mu_d c_d$ vs temperature can be ascribed to the temperature dependence of the trapping coefficient μ_d. According to the theory of Puska, Corbel, and Nieminen,[25] the temperature dependence of the positron trapping coefficient μ_d of a vacancy defect depends on the charge state of the defect. The positron trapping coefficient μ_d to a negatively charged vacancy increases as the temperature decreases, whereas the trapping coefficient μ_d to a neutral vacancy is constant as a function of temperature. When the positron trapping into the ground state of a negative vacancy takes place through a shallow Rydberg-like precursor state, the positron trapping rate can be written as[25]

$$\kappa_v(T)=\frac{\kappa_R}{1+\dfrac{\mu_R/N_{\rm at}}{\eta_R}\left(\dfrac{m^*k_BT}{2\pi\hbar^2}\right)\exp(-E_R/k_BT)}, \quad (8)$$

where $\kappa_R=\kappa_{R0}T^{-1/2}$ and $\mu_R=\mu_{R0}T^{-1/2}$ are the positron trapping rate and the trapping coefficient from the free state to the Rydberg precursor state ($\kappa_R=\mu_R c_v$), respectively, T is temperature, $N_{\rm at}$ is the atomic density of the material, η_R is the transition rate from the precursor state to the positron ground state at the vacancy, m^* is the positron effective mass, and E_R is the positron binding energy to the precursor state.

In the temperature range 150–300 K, where the divacancy is the only positron trap, it is straightforward to see from Figs. 1, 6, and 7 that κ_{V_2} increases with decreasing temperature. Equation (8) can be fitted to all data in the temperature range 150–300 K and the estimated values of the fitting parameters are $E_R=10\pm2$ meV and $\mu_{R0}/\eta_R=(6\pm2)\times10^5$ K$^{1/2}$. The temperature dependences of $\tau_{\rm ave}$, S, and W can thus be consistently explained by positron trapping at negatively charged divacancies in electron-irradiated FZ and CZ Si.

The divacancy is known to have three ionization levels $V_2^{2-/-}$, $V_2^{-/0}$, and $V_2^{0/+}$ in the band gap of Si. According to the EPR measurements of Watkins and Corbett,[19] the acceptor level $V_2^{2-/-}$ is located at $E_c-0.40$ eV and the donor level $V_2^{0/+}$ at $E_v+0.23$ eV, where E_c and E_v are the energies at the bottom of the conduction band and at the top of the valence band, respectively. The $V_2^{-/0}$ level is between these two levels, probably near the midgap. In our earlier study of proton-implanted n-type Si,[17] we observed for the divacancy a temperature dependence of the positron trapping rate that is theoretically expected for a negative defect. The positron annihilation results were in accordance with the presented level scheme: Positrons are trapped at singly negative divacancies when the Fermi level E_F has receded below $E_c-0.40$ eV. The present results are again in agreement with the this level scheme. In p-type Si the Fermi level E_F rises near the midgap after the high-fluence electron irradiation. Consequently, the $V_2^{-/0}$ electron level becomes filled and the temperature dependence of the positron trapping rate is due to the singly negative divacancies V_2^-. The filling of the $V_2^{-/0}$ level has indeed been seen in several EPR studies[19,23,24] of irradiated p-type boron-doped ([B]$=10^{15}$–10^{16} cm^{-3}) CZ Si specimens. When p-type Si is irradiated to a high electron fluence ($\geqslant10^{18}$ cm^{-2}), the EPR measurements detect the singly negative divacancy V_2^- instead of the positive divacancy V_2^+ usually seen in p-type Si by EPR.

Another level scheme is based on DLTS measurements[26] and it locates the two acceptor levels to higher energies: $V_2^{2-/-}$ at $E_c-0.23$ eV and $V_2^{-/0}$ at $E_c-0.40$ eV. According to this scheme, the divacancies in highly irradiated silicon would be neutral. Kawasuo and Okada[9] have found the pos-

itron trapping rate κ_{V_2} to decrease with temperature in accordance with our experiments. They, however, assume the charge state of the divacancy to be neutral on the basis of the DLTS level scheme. A temperature-dependent positron trapping coefficient μ_d for a neutral divacancy, however, would be difficult to understand from theoretical grounds. Also, both positron annihilation and EPR measurements detect negative divacancies in high-dose electron-irradiated p-type Si. We show below that also the illumination experiments are in accordance with the level assignments $V_2^{2-/-}$ at $E_c - 0.40$ eV and $V_2^{-/0}$ at midgap.

We estimate the divacancy concentrations from the positron trapping rates κ_{V_2} measured in darkness at 15 K (Table I) as follows. The discussion above implies that both singly negative and neutral divacancies can exist in electron-irradiated p-type Si, although the temperature dependences of $\tau_{\rm ave}$, S, and W are only due to the negative divacancy. According to experiment and theory,[8,25] the ratio $\mu_{V_2^0}:\mu_{V_2^-}:\mu_{V_2^{2-}}$ of the positron trapping coefficients of the different charge states of the divacancy is approximately 1:35:70 at 20 K. This means that at 15–20 K the positron trapping coefficient of singly negative divacancies is about one order of magnitude higher than that of neutral divacancies and the positron signal comes dominantly from the negative divacancies. By using the positron trapping coefficient $\mu_{V_2^-}=4\times10^{16}$ s^{-1} for singly negative divacancies at 15 K by Mascher, Dannefaer, and Kerr,[8] we obtain negative divacancy concentrations 4×10^{15}, 2×10^{15}, 4×10^{15}, and 2×10^{16} cm^{-3} in samples $F1$, $C1$, $C2$, and $C3$, respectively. Taking into account the neutral divacancies, the total divacancy concentrations are slightly higher. The resulting introduction rate 0.004–0.006 cm^{-1} of divacancies by 2-MeV electron irradiation is in reasonable agreement with the value $\sim$0.01 cm^{-1} given by Watkins and Corbett.[19]

The fact that the positron trapping to the vacancy-oxygen defect is observed only at temperatures below 150 K can be ascribed to the small open volume at the defect complex. The positron binding energy E_b at such center may be low. At higher temperatures the positrons trapped at the vacancy-oxygen complexes may thus escape back to the lattice. The detrapping rate $\delta_{\rm ST}$ of positrons from shallow positron traps can be written as[25]

$$\frac{\delta_{\rm ST}}{\kappa_{\rm ST}}=\frac{1}{c_{\rm ST}}\left(\frac{2\pi m^* k_B T}{h^2}\right)^{3/2}\exp\left(-\frac{E_b}{k_B T}\right), \tag{9}$$

where $\kappa_{\rm ST}$ is the trapping rate to the shallow trap and $c_{\rm ST}$ is the shallow trap concentration. In CZ Si the temperature dependence of the average lifetime can be quantitatively modeled with Eq. (9) as in Ref. 5. The analysis yields the positron binding energy of $E_b=40\pm4$ meV at the vacancy-oxygen defect.

This behavior was also found by Mascher, Dannefaer, and Kerr[8] in their positron lifetime measurements of electron-irradiated n-type Si. They assigned a lifetime of $\tau_d=225$ ps for the shallow positron traps detected in their experiments and they associated the traps to the A centers. Their value 225 ps is, within error bars, the same as the positron lifetime $\tau_{d2}=230(10)$ ps we obtain in this work. In addition, we have shown by Doppler-broadening measurements that the defect indeed contains oxygen.

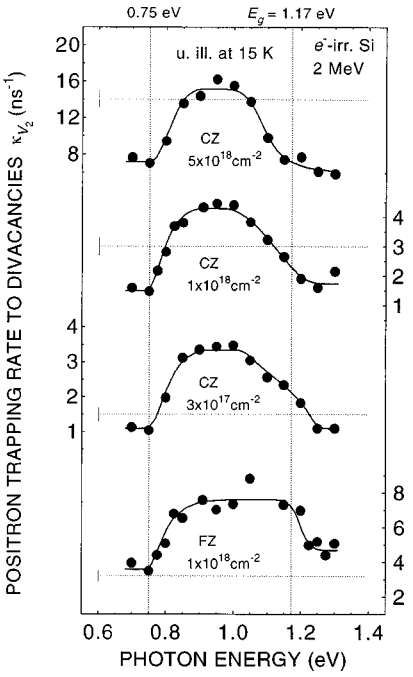

FIG. 8. Positron trapping rate κ_{V_2} to divacancies in electron-irradiated FZ Si (sample $F1$) and CZ Si (samples $C1-C3$) at 15 K under illumination with monochromatic light. The dotted horizontal lines indicate the values of κ_{V_2} in darkness at 15 K. The solid lines are guides to the eye.

V. PHOTOIONIZATION OF DIVACANCY

In the following we discuss the changes in divacancy concentrations observed by positron annihilation measurements under illumination at 15 K and the optical processes involved.

A. Positron trapping rate to divacancies under illumination

As shown in Fig. 8, the positron trapping rate κ_{V_2} to divacancies under illumination at 15 K has a photon energy dependence similar to the average positron lifetime presented above in Fig. 2. We observe the following features. First, when the photon energy $h\nu$ increases above 0.75 eV, κ_{V_2} increases rapidly and levels off at about 0.90 eV. Second, near the band-gap energy κ_{V_2} decreases again. In CZ Si this decrease begins at 1.0 eV and it seems to be more rapid when the irradiation fluence increases. Third, in FZ Si the $\kappa_{V_2}(h\nu)$ curve is above the value $\kappa_{V_2}^{\rm dark}$ measured in darkness, but in CZ Si $\kappa_{V_2}(h\nu)$ is partly below $\kappa_{V_2}^{\rm dark}$. The downshift of $\kappa_{V_2}(h\nu)$ with respect to $\kappa_{V_2}^{\rm dark}$ in CZ Si increases with increasing irradiation fluence.

To understand the changes in the positron trapping rate $\kappa_{V_2}(h\nu)$ under illumination at 15 K we need to consider the fact that the divacancies can exist in different charge states V_2^q. We write the total positron trapping rate to divacancies as $\kappa_{V_2}=\Sigma_q\mu_{V_2^q}[V_2^q]$. As the individual trapping coefficients $\mu_{V_2^q}$ are not affected by illumination, we see that the changes

in κ_{V_2} under illumination are due to changes in the concentrations $[V_2^q]$. In other words, the illumination changes the occupations of the charge states of the divacancy from those in darkness. Below we shall examine the mechanisms responsible for this effect.

B. Photoionization and charge states of the divacancy

Photoillumination can, in theory, change the charge states of the divacancies either by optical electron and hole emission from the electron levels of the divacancies or by capture of photogenerated electrons and holes on the electron levels of the divacancy. We ascribe the ionization of divacancies in the photon energy range 0.70–1.0 eV to direct optical electron and hole emission processes on the basis of the following experimental observations.

(i) In the photon energy range 0.70–1.0 eV, the $\kappa_{V_2}(h\nu)$ curve has a shape that is characteristic of the optical ionization cross section of a deep level defect.[27] The optical electron and hole-emission cross sections $\sigma(h\nu)$ increase sharply when the photon energy increases above a threshold energy E_i. The energy E_i can be the distance of the defect electron level from either the conduction-band minimum E_c or from the valence-band maximum E_v. In Fig. 8 we observe such a threshold energy at 0.75 eV. The shape of the $\kappa_{V_2}(h\nu)$ curve can also be characterized by the ratio of κ_{V_2} measured under 0.95-eV illumination to that under 0.70-eV illumination. We see that in all samples $F1$ and $C1-C3$ this ratio is, within error bars, approximately 2. The similarity of the shapes of $\kappa_{V_2}(h\nu)$ in different materials and after different irradiations suggests that this shape arises from an optical cross section $\sigma(h\nu)$ rather than from carrier capture. We attribute the threshold energy 0.75 eV to an electron level of the divacancy. The increase of the positron trapping rate $\kappa_{V_2}(h\nu)$ above 0.75 eV means that divacancies are converted to a more negative charge state.

(ii) We observed that under 0.95-eV illumination (Fig. 4), the effect of illumination on the positron annihilation signals is in saturation at the photon flux $1\times10^{16}\ \mathrm{cm^{-2}\,s^{-1}}$. Such a saturation suggests that at this photon energy and flux, optical ionization processes dominate whereas the effect of carrier capture is small. Photogeneration of carriers by ionizing another defect than the divacancy would, just like the ionization of the divacancy, have a threshold energy. Thus, if photogeneration and trapping of carriers are not observed at 0.95 eV, they also will not contribute at photon energies lower than 0.95 eV.

(iii) The positron trapping rate ratios $\kappa_{V_2}(0.70\ \mathrm{eV})/\kappa_{V_2}^{\mathrm{dark}})$ and $\kappa_{V_2}(0.95\ \mathrm{eV})/\kappa_{V_2}^{\mathrm{dark}}$ (which can be calculated from Fig. 5 for samples $C2$ and $F1$) remain approximately unchanged when the temperature increases from 15 to 60 K. This means that under the illuminations between 15 and 60 K, the concentrations of differently charged divacancies do not depend on temperature. If the light-induced changes in divacancy concentrations were due to carrier trapping, one would expect the changes to depend strongly on temperature.

It is thus fair to say that at 15 K, under illumination at photon energies below 1.0 eV and with a flux of $1\times10^{16}\ \mathrm{cm^{-2}\,s^{-1}}$, only optical ionization processes determine the charge-state balance of the divacancy. As discussed below in Sec. V C, carrier capture processes become important in CZ Si when the photon energy is above 1.0 eV.

C. Identities of the optical processes

We now identify the processes involved in the ionization of divacancies and discuss the relation of these processes to the electron level scheme of the divacancy. We show that the features in the $\kappa_{V_2}(h\nu)$ curves can be explained by optical ionization of the $V_2^{-/0}$ and $V_2^{2-/-}$ electron levels of the divacancy. We proceed by analyzing the different photon energy ranges in Fig. 8.

1. 0.70–0.75 eV

Experimentally, the illumination at the photon energies 0.70–0.75 eV changes the positron trapping rate at negative divacancies. In principle, the difference between κ_{V_2} and $\kappa_{V_2}^{\mathrm{dark}}$ in this energy range could thus be attributed to the photoionization of either the $V_2^{-/0}$ or the $V_2^{2-/-}$ levels of the divacancy. However, since we detect another ionization level of the negative divacancy at higher photon energies 0.75–1.0 eV (see below), the illumination effects at 0.70–0.75 eV can only be due to the photoionization of the $V_2^{-/0}$ level. We denote the optical electron and hole-emission cross sections of the $V_2^{-/0}$ level by the symbols $\sigma_n^{-/0}$ and $\sigma_p^{-/0}$, respectively. Under illumination in steady-state condition, the concentration ratio of singly negative and neutral divacancies changes from the thermal equilibrium to $\{[V_2^-]/[V_2^0]\}_{h\nu}=\sigma_p^{-/0}/\sigma_n^{-/0}$, which is independent of the sample.[27] The downshift of κ_{V_2} below $\kappa_{V_2}^{\mathrm{dark}}$ is easily understood as follows. In darkness, the Fermi level E_F is near the divacancy level $V_2^{-/0}$ at $\sim E_g/2$ and both singly negative and neutral divacancies coexist in all samples. The Fermi level E_F and the concentration ratio $\{[V_2^-]/[V_2^0]\}_{\mathrm{dark}}$ in darkness increase with the electron-irradiation fluence. The decrease of $\kappa_{V_2}(h\nu)$ with respect to $\kappa_{V_2}^{\mathrm{dark}}$ is thus due to the fact that the ratio $\{[V_2^-]/[V_2^0]\}_{h\nu}$ becomes smaller than the value $\{[V_2^-]/[V_2^0]\}_{\mathrm{dark}}$. This result is in agreement with the idea discussed in Sec. IV B 3 that in p-type Si the $V_2^{-/0}$ level of the divacancy becomes more filled when the irradiation fluence increases.

2. 0.75–1.00 eV

As mentioned above in Sec. V B, this part of the $\kappa_{V_2}(h\nu)$ curve is ascribed to the energy dependence of the optical hole emission from a negative level of the divacancy at $E_v+0.75$ eV. As the ionization of the $V_2^{-/0}$ is observed already below 0.75 eV, the level at $E_v+0.75$ eV must then be the $V_2^{2-/-}$ level and the shape of $\kappa_{V_2}(h\nu)$ between 0.75 and 1.00 eV is due to the optical hole-emission cross section $\sigma_p^{2-/-}$ of the $V_2^{2-/-}$ level. This result is in agreement with the level scheme presented in Sec. IV B 3, according to which the divacancy $V_2^{2-/-}$ level is at $E_c-0.40$ eV.

3. 1.00–1.25 eV

In FZ Si, $\kappa_{V_2}(h\nu)$ remains constant up to the band-gap energy E_g. In CZ Si, $\kappa_{V_2}(h\nu)$ starts to decrease at a photon

energy of 1.0 eV and the decrease becomes steeper with increasing irradiation fluence. This decrease continues smoothly to photon energies above the band edge, which suggests that the effect is not an intrinsic property of the divacancy or any other defect. It rather reflects the high overall defect density in high-fluence electron-irradiated CZ Si. This may cause the deformation of the band edge, which is seen as trapping of carriers generated with sub-band-gap energies. Such absorption tails that can extend to photon energies down to 0.8 eV have been seen in photoconductivity measurements of Si irradiated with 1.5-MeV electrons to high electron fluences ($\geqslant 10^{18}$ cm^{-2}).[28]

4. 1.25–1.30 eV

Above the band-gap energy E_g, the light is obviously absorbed and the dominant optical process is the generation of electron-hole pairs. The charge states of the divacancies are then determined by carrier-capture processes. For example, considering only the $V_2^{-/0}$ level, the occupancy ratio of the level becomes $\{[V_2^-]/[V_2^0]\}_{h\nu}=c_n n/c_p p$, where c_n and c_p are the electron and hole capture cross sections and n and p are the electron and hole concentrations, respectively. The net effect in FZ Si seems to be the electron capture, whereas in CZ Si it is the hole capture.

D. Discussion and comparison with other studies

The important consequence of the illumination experiment is that the $V_2^{-/0}$ ionization level of the divacancy must be lower than 0.40 eV below the conduction-band minimum. The DLTS level scheme (see Sec. IV B 3), where the $V_2^{-/0}$ level is at $E_c-0.40$ eV, cannot explain the changes in the positron trapping rate κ_{V_2} under illumination with photon energies below 0.75 eV. On the other hand, our results are fully consistent with the EPR level scheme, where the $V_2^{-/0}$ level is at $\sim E_g/2$ and the $V_2^{2-/-}$ level is at $E_c-0.40$ eV.

It is also interesting to note that in the photoconductivity measurements of Young and Corelli[29] an electron level of the divacancy was detected at a photon energy of 0.75 eV. The photoconductivity signal was associated with the electron emission from the $V_2^{0/+}$ level. We observe by positron annihilation an electron level of the divacancy at the same photon energy of 0.75 eV and we have shown that the optical process can be ascribed to the hole emission from the $V_2^{2-/-}$ level of the divacancy.

The contribution of the $V_2^{0/+}$ ionization level is less clearly seen in the $\kappa_{V_2}(h\nu)$ curve. The shape of the $\kappa_{V_2}(h\nu)$ curve may, however, indirectly imply the ionization of $V_2^{0/+}$. According to the simple model by Lucovsky,[27] the optical ionization cross sections of deep levels are expected to increase steadily between the ionization threshold E_i and $2E_i$. However, the $\kappa_{V_2}(h\nu)$ curve, the shape of which in our experiments between 0.75 and 1.0 eV reflects mainly the hole emission cross section $\sigma_p^{2-/-}$, levels off in all samples already at 0.90 eV. This could be due to the onset of the optical electron emission from the $V_2^{0/+}$ level at $E_v+0.23$ eV. In earlier IR absorption measurements,[30] the optical hole emission from the $V_2^{0/+}$ level has been observed. A more comprehensive view of the ionization of the $V_2^{0/+}$ level could be obtained by combining positron annihilation with IR absorption measurements.

VI. CONCLUSIONS

Vacancies and their photoionization were investigated in 2-MeV electron-irradiated silicon by positron annihilation spectroscopy. To introduce pure vacancies and vacancy-oxygen defects, we irradiated at room-temperature FZ Si ($\rho=10^4$ Ω cm and [O]$\leqslant 10^{15}$ cm^{-3}) and CZ Si ($\rho=8-15$ Ω cm and [O]$=10^{18}$ cm^{-3}) samples to electron fluences of $(3\times10^{17})-(5\times10^{18})$ cm^{-2}.

Upon the electron irradiation at room temperature, we observed negative and neutral divacancies in both FZ and CZ Si. The characteristic positron lifetime and the characteristic low [for $p_z=(0-2.8)\times10^{-3}m_0c$] and high-momentum [for $p_z=(11-20)\times10^{-3}m_0c$] parameters of the divacancy are determined as $\tau_{d1}=300(5)$ ps$=1.35(2)\times\tau_b$, $S_{d1}=1.055(3)\times S_b$, and $W_{d1}=0.75(2)\times W_b$, respectively.

Illumination with (0.70–1.30)-eV monochromatic light has a strong effect on the positron trapping to the divacancy at 15 K. Depending on the photon energy, the positron trapping to divacancies can be enhanced or reduced by illumination and the maximum amplitude of changes in the positron lifetime is 15 ps. The results can be understood in terms of optical electron and hole emission from the electronic levels $V_2^{-/0}$ and $V_2^{2-/-}$ of the divacancy. The photoionization changes the populations of the neutral, singly negative, and doubly negative divacancies. The spectral changes in the positron trapping rate are due to the different sensitivities of the positron to detect V_2^0, V_2^-, and V_2^{2-}. The spectral shape of the positron trapping rate reveals an electron level of the divacancy at $E_v+0.75$ eV. We assign this level to the ionization level $V_2^{2-/-}$ of the divacancy. The $V_2^{-/0}$ level must be below this energy and we find it to be at about midgap.

In addition to the divacancy, we observed positron trapping to oxygen-related defects, particularly in CZ Si. The detected vacancy-oxygen complex has a small open volume [$\tau_{d2}=230(10)$ ps$=1.04(4)\times\tau_b$] and the decoration by oxygen is revealed by the broad momentum distribution [$S_{d2}=0.984(3)\times S_b$ and $W_{d2}=1.16(4)\times W_b$]. The defect complex is probably the A center.

*Present address: Laboratory of Physics, Helsinki University of Technology, P.O. Box 1100, FIN-02015 HUT, Finland.

†Present address: DRECAM/SCM, Laboratoire CEA de Radiolyse, 91191 Gif-sur-Yvette Cedex, France.

[1] G. D. Watkins, in *Deep Centers in Semiconductors*, edited by S. T. Pantelides (Gordon and Breach, New York, 1986), p. 147.

[2] F. Bridges, G. Davies, J. Robertson, and A. M. Stoneham, in *Current Issues in Condensed Matter Spectroscopy*, edited by A. M. Stoneham (Hilger, Bristol, 1990), p. 9.

[3] P. Hautojärvi and C. Corbel, in *Positron Spectroscopy of Solids*, edited by A. Dupasquier and A. P. Mills, Jr. (IOS, Amsterdam, 1995), pp. 491 and 533.

[4] M. J. Puska and R. M. Nieminen, Rev. Mod. Phys. **66**, 841 (1994).

[5] K. Saarinen, P. Hautojärvi, and C. Corbel, in *Identification of Defects in Semiconductors*, edited by M. Stavola (Academic, New York, in press).
[6] P. Asoka-Kumar, K. G. Lynn, and D. O. Welch, J. Appl. Phys. **76**, 4935 (1994).
[7] J. Mäkinen, C. Corbel, P. Hautojärvi, P. Moser, and F. Pierre, Phys. Rev. B **39**, 10 162 (1989); J. Mäkinen, P. Hautojärvi, and C. Corbel, J. Phys.: Condens. Matter **4**, 5137 (1992).
[8] P. Mascher, S. Dannefaer, and D. Kerr, Phys. Rev. B **40**, 11 764 (1989).
[9] A. Kawasuo and S. Okada, Jpn. J. Appl. Phys., Part 1 **36**, 605 (1997).
[10] A. Polity, S. Huth, and R. Krause-Rehberg, Mater. Sci. Forum **255–257**, 602 (1997).
[11] Z. Tang, M. Hasegawa, T. Chiba, M. Saito, A. Kawasuo, Z.-Q. Li, R. T. Fu, T. Akahane, Y. Kawazoe, and S. Yamaguchi, Phys. Rev. Lett. **78**, 2236 (1997).
[12] S. Szpala, P. Asoka-Kumar, B. Nielsen, J. P. Peng, S. Hayakawa, K. G. Lynn, and H.-J. Gossmann, Phys. Rev. B **54**, 4722 (1996).
[13] J. Kuriplach, T. Van Hoecke, B. Van Wayenberge, C. Dauwe, D. Segers, N. Balcaen, A. L. Morales, M.-A. Trauwert, J. Vanhellemont, and M. Sob, Mater. Sci. Forum **255–257**, 605 (1997).
[14] K. Saarinen, S. Kuisma, P. Hautojärvi, C. Corbel, and C. LeBerre, Phys. Rev. Lett. **70**, 2794 (1993).
[15] S. Kuisma, K. Saarinen, P. Hautojärvi, C. Corbel, and C. LeBerre, Phys. Rev. B **53**, 9814 (1996).
[16] K. Saarinen, P. Hautojärvi, P. Lanki, and C. Corbel, Phys. Rev. B **44**, 10 585 (1991).
[17] H. Kauppinen, C. Corbel, K. Skog, K. Saarinen, T. Laine, P. Hautojärvi, P. Desgardin, and E. Ntsoenzok, Phys. Rev. B **55**, 9598 (1997).
[18] M. Hakala, M. J. Puska, and R. M. Nieminen (unpublished).
[19] G. D. Watkins and J. W. Corbett, Phys. Rev. **138**, A543 (1965); J. W. Corbett and G. D. Watkins, *ibid.* **138**, A555 (1965).
[20] G. D. Watkins and J. W. Corbett, Phys. Rev. **121**, 1001 (1961).
[21] V. Avalos and S. Dannefaer, Phys. Rev. B **54**, 1724 (1996).
[22] S. Dannefaer and D. Kerr, J. Appl. Phys. **60**, 1313 (1986).
[23] Y. H. Lee, J. W. Corbett, and K. L. Brower, Phys. Status Solidi A **41**, 637 (1977).
[24] Y. H. Lee, J. W. Corbett, and K. L. Brower, Phys. Rev. B **13**, 2653 (1976).
[25] M. J. Puska, C. Corbel, and R. M. Nieminen, Phys. Rev. B **41**, 9980 (1990).
[26] A. O. Evwaraye and E. Sun, J. Appl. Phys. **47**, 3776 (1976).
[27] P. Blood and J. W. Orton, *The Electrical Characterization of Semiconductors: Majority Carriers and Electron States* (Academic, London, 1992), p. 682.
[28] A. H. Kalma and J. C. Corelli, Phys. Rev. **173**, 735 (1968).
[29] R. C. Young and J. C. Corelli, Phys. Rev. B **5**, 1455 (1972).
[30] L. J. Cheng, J. C. Corelli, J. W. Corbett, and G. D. Watkins Phys. Rev. **152**, 761 (1966).
[31] J. Keinonen, M. Hautala, E. Rauhala, V. Karttunen, A. Kuronen, J. Räisänen, J. Lahtinen, A. Vehanen, E. Punkka, and P. Hautojärvi, Phys. Rev. B **37**, 8269 (1988).
[32] R. Ambigapathy, A. Manuel, P. Hautojärvi, K. Saarinen, and C. Corbel, Phys. Rev. B **50**, 2188 (1994).